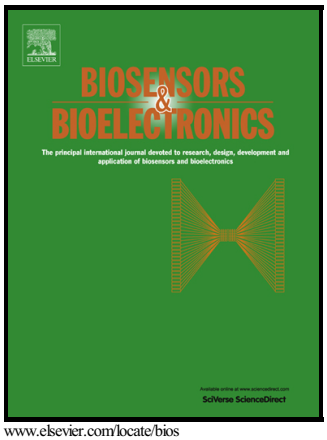

www.elsevier.com/locate/bios

Highly sensitive electrochemical detection of genomic DNA based on stem loop probes structured for magnetic collection and measurement via metalised hollow polyelectrolyte Shells

Naphat Khunrattanaporn, Patsamon Rijiravanich, Mithran Somasundrum, Werasak Surareungchai

PII: S0956-5663(15)30163-9
DOI: http://dx.doi.org/10.1016/j.bios.2015.05.068
Reference: BIOS7732

To appear in: *Biosensors and Bioelectronic*

Received date: 11 February 2015
Revised date: 27 May 2015
Accepted date: 28 May 2015

Cite this article as: Naphat Khunrattanaporn, Patsamon Rijiravanich, Mithran Somasundrum and Werasak Surareungchai, Highly sensitive electrochemical detection of genomic DNA based on stem loop probes structured for magnetic collection and measurement via metalised hollow polyelectrolyte Shells, *Biosensors and Bioelectronic,* http://dx.doi.org/10.1016/j.bios.2015.05.068

Highly Sensitive Electrochemical Detection of Genomic DNA Based on Stem Loop Probes Structured for Magnetic Collection and Measurement via Metalised Hollow Polyelectrolyte Shells

Naphat Khunrattanaporn,[1] Patsamon Rijiravanich,[2] Mithran Somasundrum,[2,*] Werasak Surareungchai[1,*]

[1]*School of Bioresources and Technology, King Mongkut's University of Technology Thonburi, Bang Khun Thian, Bangkok 10150, Thailand*

[2]*Biochemical Engineering and Pilot Plant Research and Development Unit, National Center for Genetic Engineering and Biotechnology, National Science and Technology Development Agency at King Mongkut's University of Technology Thonburi, Bang Khun Thian, Bangkok 10150, Thailand*

[*]Authors for correspondence: mithran.somasundrum@gmail.com, werasak.sur@kmutt.ac.th

ABSTRACT

We report a highly sensitive method for the electrochemical detection of genomic DNA, based on the employment of two sub-micron oligonucleotide labels -- one for magnetic collection and the other for voltammetric detection -- and their incorporation onto a stem loop DNA probe. The magnetic label consists of a latex particle of mean diameter 441 + 6 nm, bearing magnetic Fe_3O_4 particles and approx. 3.5×10^5 anti-DIG antibodies. The voltammetric label is a hollow polyelectrolyte shell containing approx. 1.0×10^{11} Au atoms in the form of well dispersed Au nanoparticles. A DIG tag on one arm of the stem loop enables binding to the magnetic label, while a thiol tag on the other arm enables attachment to the Au nanoparticles. Due to steric hindrance from the two relatively large labels, attachment of both moieties is dependent on target - probe hybridisation straightening the loop. Once attached, sensitive DNA measurement is facilitated by magnetic collection of the DNA into a small volume and by the high quantity of Au atoms available for detection. Using differential pulse anodic stripping voltammetry we calibrated a 30 mer sequence common to 71 strains of *E. coli* across the concentration range 0.1 aM to 100 pM with a LOD of 1.8 aM. Three strains of *E. coli*, BL 21, ATCC8739, O157:H7, when spiked into UHT milk and fermented palm juice, could be detected with LODs of approx. 2 - 4 CFU mL^{-1} in an assay time of approx. 140 min.

Keywords: DNA Biosensor; E. coli; Latex; Voltammetry; Nanoparticle

1. Introduction

The detection of specific DNA sequences is relevant to many analytical applications, including the sensing of viruses, pathogenic microorganisms, food borne bacteria, biological warfare agents and the identification of human genetic diseases (Davis and Higson, 2012; Ozsoz, 2012; Palecek and Fojta, 2005). In many of these applications the DNA concentration to be measured is very low and therefore the assay sensitivity needs to be high. The sensitivity of a given technique can be improved by using the polymerase chain reaction (PCR) to amplify the DNA sample, but this requires expensive equipment and trained personnel. Electrochemistry is of interest in this context. In the case of voltammetric detection of an electrochemical label, there is scope for achieving highly sensitive detection through label design, while at the same time using relatively inexpensive equipment. The label signaling species can be an enzyme involved in the generation of an electroactive product (Cheng et al., 2014; Sun et al., 2015), a redox molecule that intercalates to the nucleic acid duplex (Li et al., 2007) or associates with the anionic phosphate groups (Zhu et al., 2009), graphene oxide nanoplatlets (Bonami et al., 2012), or a metal nanomaterial in the form of a particle (Authier et al., 2000; Wang et al., 2001a), nanorod (Wang et al., 2003a), or quantum dot (Dong et al., 2010; Hansen et al., 2006). The use of metal nanoparticles is attractive due to the fact that they offer chemical stability and can be detected at high

sensitivities through the preconcentration step of anodic stripping voltammetry (ASV). Increasing the sensitivity of such labeling essentially consists of increasing the quantity of nanomaterial associated with each binding event. (For recent reviews see Wu et al., 2014 and Chen and Chaterjee, 2013). Hence, since the initial method of attaching individual nanoparticles to oligonucleotide sequences (Authier et al., 2000; Wang et al., 2001a), strategies have been developed to attach nanoparticle assemblies. This has been through loading the nanoparticles on a solid support such as latex particles (Dong et al., 2010; Pinijsuwan et al., 2008) or carbon nanotubes (Wang et al., 2003b; Wang et al., 2013), the use of catalytic reduction to increase the quantity of nanomaterial on the label (Taton, et al., 2000; Wang et al., 2001b; Lin et al., 2011), the association of positively charged Ag nanoparticles with the negative phosphate groups of DNA (Zhang et al., 2009), or the formation of nanoparticle aggregates, caused by target - probe binding (Li et al., 2010). We previously achieved a LOD of approx. 25 fM (Rijiravanich et al., 2008) using spherical sub-micron latex particles as ultimately dissolved templates, to construct hollow polyelectrolyte shells which were then loaded with Ag nanoparticles by using changes in pH to open and close the capsules. Control experiments indicated that most of the Ag nanoparticles were located on the inner capsule walls (Rijiravanich et al., 2008), which implied a much higher nanomaterial loading could be achieved given a means of fixing particles into the central volume of the capsules. We wish to report here a new, related, platform and its application to the detection of genomic DNA, based on significant improvements to our previous strategy. Firstly, by adapting a seed-mediated growth technique, previously used for modifying solid particles (Sanchez-Gaytan and Park, 2010), in conjunction with entrapment in the capsules of short chain polyallylamine (PAA) as a sorption material, we have been able to greatly increase the quantity of nanometal

bound per capsule. Secondly, we performed target binding with a stem loop probe structured to enable magnetic collection into a small volume. The combination of these two things enabled us to record a low limit of detection (LOD) for a target sequence in buffer solution and for three strains of *E. coli* spiked into milk and fermented palm juice.

2. Experimental

2.1 Chemicals

All reagents were analytical grade and used without further purification. The commercial genomic DNA extraction kit was purchased from RBC Bioscience Lab (Taiwan). The commercial protein assay was from Bio-Rad Laboratories Ltd. Polystyrene-co-acrylic acid (PSA) particles were synthesised according to Pinijsuwan et al. (2008). All stock solutions were prepared using sterile Milli-Q water (resistance > 18.2 MΩ). The synthetic oligonucleotide sequences were stored frozen and had the following sequences: stem loop probe, SH-$(CH_2)_6$-5'-AAA ggC CgT CTT CCT gAg TAA TAA CTT CCT gAg TgA ATA ACg gCC AAA) -3'-DIG (Gene Link, USA); target, 5'-TAT TCA CTC AGG AAG TTA TTA CTC AGG AAG-3' (Thermo Scientific, Germany); one base mismatch, 5'-TAT TCA CTC AGC AAG TTA TTA

CTC AGG AAG-3’ (Thermo Scientific, Germany); three base mismatch, 5’-TAT TCA CTC AGC AAC TTA TTA CTC ACG AAG-3’ (Thermo Scientific, Germany); non-complementary strand, 5’-AGT AAT GGA ACG GTT GCT CTT TTC ATT TAG CTT TGT TAG CGT TAG GTA TAT -3’

(Bio Basic Inc., US)*2.2 Apparatus*

Differential pulse anodic striping voltammetry (DPASV) was performed with an Autolab PGSTAT 10 computer-controlled potentiostat (Ecochemie, Netherlands) using GPES software. Transmission electron micrographs were obtained with a JEOL model JM-2100 TEM (accelerating voltage 120 kV). Scanning electron microscopy and field-emission scanning electron microscopy was performed with a JEOL model JSM-6300 SEM, and a Hitachi model S-4700 FE-SEM, respectively. UV-visible spectroscopic measurement was carried out on a Beckman model DU-7000 or a microplate reader model Tecan M200. DNA concentrations were measured with a Nanodrop spectrophotometer model ND100. Carbon track screen-printed electrodes (SPEs) were fabricated in-house with a working area at 1.5mm × 4 mm, and were used with a commercial Ag/AgCl (3M NaCl) reference half cell and Pt coil counter electrode.

2.3 Procedures

Hollow polyelectrolyte capsules were prepared from a previous method with some modifications (Rijiravanich et al., 2008). Short chain PAA was loaded into the capsules by manipulation of pH using H_2SO_4 for capsule opening and NaOH for capsule closing. Seed decoration of the PAA loaded capsules was performed by loading $AuCl_4^-$ ions onto the positively charged PAA, followed by reduction to Au metal using $NaBH_4$. The seed-decorated capsules were metalised by the procedure of Sanchez-Gaytan and Park (2010), using ascorbic acid in the presence of CTAB as the reducing agent. Anti-DIG modified magnetic latex was prepared by coating magnetic Fe_3O_4 particles with APTS to impart a positive charge and these were then bound to negatively charged PSA latex by electrostatic attraction. Stock cell cultures (*E. coli* BL21, ATCC8739, O157:H7 and *Salmonella enterica serovar* Typhimurium) were incubated in nutrient broth under rotary shaking, collected by and stored in phosphate buffer at 4^{o}C. Cell numbers were determined by the standard serial dilution, plating onto nutrient agar technique. Genomic DNA was extracted either by heat shock using incubation at 100 ^{o}C or a commercial extraction kit. (See Supporting Information for full details of all the above procedures.)

3. Results and Discussion

3.1 Construction of Hollow Polyelectrolyte Shell Labels

To use as templates for capsule construction we synthesised polystyrene-coacrylic acid (PSA) particles. These were spherical in shape, well dispersed in aqueous solution and had a mean diameter of 441 nm + 6 nm (n = 42) from TEM. Deposition of 4 PAA/PSS bilayers onto the spheres by a layer-by-layer process (Decher and Hong, 1991) resulted in the mean particle diameter increasing to 465 nm + 7 nm (n = 42) (for TEM images see Supporting Information, Fig. S-1). Dissolution of the PSA templates by THF then produced hollow polyelectrolyte shells. Template removal caused the polyelectrolyte layer to shrink down to a somewhat oval shape, with a corresponding increase in capsule wall thickness (from 23 nm + 9 nm to 48 nm + 4 nm, n = 5, see Supporting Information, Fig. S-1). Using pH-assisted opening (< pH 4) and closing (> pH 8), we incorporated short chain PAA (MW ~ 15,000) within the capsules. To estimate the uptake of short chain PAA we measured UV absorbance at 210 nm. A calibration curve for PAA was plotted at this wavelength across the concentration range 0.1 to 10 μg μL^{-1} (y (Abs) = 0.4675 c (μg μL^{-1}) - 0.0003, r^2 = 0.999, n = 13) and this curve was then used to determine the change in PAA concentration after uptake and removal of the hollow capsules. To enable us to estimate the capsule concentration we treated the structures as spheres and measured the mean outer (r_{out}) and inner (r_{inn}) radii from TEM images (n = 5). The capsule thickness is thus approximated to $(4/3)\pi(r^3_{out} - r^3_{inn})$. Assuming a polyelectrolyte shell density of 1.1 g cm^{-3} (Rijiravanich et al., 2004), we can approximate a shell mass of 2.4×10^{-14} g. From this value we converted the dry mass of a known aliquot volume of capsules to a concentration. From UV absorbance, exposure to a quantity of 1.05×10^{12} capsules caused a total uptake of 0.14 g short chain PAA. This corresponds to an incorporation of approx. 1.3×10^{-13} g PAA per capsule, i.e. an

increase in capsule mass of approx. 5.5 times. Given that TEM images of post-loaded capsules (Supporting Information, Fig. S-1) showed essentially no change in wall thickness within the precision of the measurement (49 nm + 2 nm, $n = 5$), it is reasonable to conclude most of the short chain PAA was dispersed within the capsule centres.

Au nanoparticles were loaded into the polyelectrolyte shells using seed-mediated growth. This technique has previously been used to create metal nanoshells around solid particles for uses such as surface plasmon excitation (Hirsch et al., 2006). The concept is that a core is functionalised with metal nanoparticles which then act as sites for further metal reduction, enabling uniform coverage. Here we report for the first time that seed mediated growth can be used to modify hollow polyelectrolyte shells. We used a version of the method Sanchez-Gaytan and Park (2010) described to deposit Au around polystyrene-PAA particles. Initial seeding was performed by exposing the PAA-loaded capsules to $HAuCl_4$ (a TEM of a seeded capsule is shown in Fig. 1(a)). We expect the negative $AuCl_4^-$ ions to associate with the positive PAA both in the capsule walls and dispersed within the capsule centre. To quantify the Au taken up by the capsules we used: 1) Change in UV absorbance of $HAuCl_4$ solution at 294 nm, using a linear calibration following the equation: y (Abs) = 4.0326c (mM) - 0.1363, ($r^2 = 0.994$, $n = 10$). 2) Removal and washing of the capsules followed by acid dissolution and then detection by differential pulse anodic stripping voltammetry (DPASV), using a calibration curve following the equation y (I_{pk}) = 1.0×10^{-6} c (M) - 3×10^{-7}, ($r^2 = 0.9952$, $n = 15$). (Examples of differential pulse voltammograms for the detection of $HAuCl_4$ solution and of Au-loaded PAA capsules are given in Supporting Information, Fig. S-2). UV quantification of the unencapsulated $AuCl_4^-$ implied a steadily increasing degree of $AuCl_4^-$ uptake into the capsules, up to extremely high bulk

concentrations of $HAuCl_4$ (> 1.2 M, see Supporting Information, Fig. S-3). This was contradicted by the DPASV result which indicated an optimum Au loading was achieved at a bulk $HAuCl_4$ concentration of 0.2 M (see Supporting Information, Fig. S-4). This is likely to be because the DPASV result includes the effect of excess unreduced $AuCl_4^-$ being removed by the three centrifugation/removal/redispersion washing cycles. The UV measurement does not distinguish between $AuCl_4^-$ reduced to Au atoms and $AuCl_4^-$ lost to solution.

To deposit further Au onto the seeded capsules we used a growth solution of CTAB, $HAuCl_4$ and ascorbic acid, as adapted from Sanchez-Gaytan and Park (2010). We increased the solution volume (from 1 mL to 10 mL) for a fixed quantity of seed-decorated capsules, thereby increasing the Au : capsule ratio. Quantification of the amount of Au incorporated into each preparation was by DPASV, following washing and re-dispersion (see Fig. 2). We also TEM imaged each capsule preparation (Fig. 1 (b) - (f)). It can be seen from Fig. 2 that the quantity of Au incorporated (expressed as Au atoms per capsule, using the previously estimated capsule concentration) increased with increasing Au : capsule ratio, which is a commonsense result. However, the TEM images show that high Au loadings essentially tear the capsules into fragments. We chose a 5 mL growth solution volume (Fig. 1(d)) as giving the highest Au loading while retaining capsule integrity. From Fig. 2 this provides a loading of 1.0×10^{11} Au atoms per capsule, which represents an increase in nanomaterial per label by four orders of magnitude over our previous method of capsule loading (Rijiravanich et al., 2008. Approx. 2.8×10^7 Ag atoms per capsule, based on an estimated loading of 78 Ag nanoparticles per capsule, mean Ag nanoparticle diameter = 22. 7 nm, using Ag density = 10.49 g cm^{-3}. (www. webelements.com)

3.2 Construction of Magnetic, Anti-DIG Modified Latex

As shown in Scheme 1, our detection system is based on the concept that attachment of the magnetic collection label to one arm of the unhybridised stem loop renders the other arm sterically inaccessible to the electrochemical label, thereby allowing only hybridised stem loop probes to be labeled. For this situation to be realised the magnetised particle needs to be relatively large. To meet this criteria we adapted a form of magnetic labeling previously developed for a biobarcode immunoassay (Pratiwi et al., 2013). This used magnetic Fe_3O_4 particles coated with the silane APTS. At pH <8 the amino group of APTS is protonated, imparting a positive charge (Zhang, S. et al., 2009). Hence, the coated Fe_3O_4 could be electrostatically attached to negatively charged PSA latex particles. One stem loop arm contained a DIG tag, while anti-DIG antibodies were attached to the magnetic latex. The anti-DIG antibody was a fab fragment labeled with alkaline phosphatase (AP). The enzyme enabled adsorption to the positively charged APTS-coated Fe_3O_4 by electrostatic attraction (AP PI = 4.5, Tadera et al., 2003) and could be used to test for successful connection to magnetic latex by colorimetric observation of *p*-nitrophenol, following AP-catalysed dephosphorylation of the substrate *p*-nitrophenyl phosphate (*p*NPP). We found that the characteristic yellow colour of *p*-nitrophenol was clearly observed when exposing anti-DIG modified magnetic latex to *p*NPP, but not in the absence of either anti-DIG or *p*NPP (see Supporting Information Fig. S-5). Using the Bradford test on the supernatant following exposure and then removal of the labels, we estimate a loading of 3.5×10^5 anti-DIG

antibodies per magnetic latex particle. Modification of the latex by Fe_3O_4/anti-DIG could be visualised by SEM as an increased surface roughness (see Supporting Information Fig. S-6).

3.3 Detection of DNA Hybridisation

As shown in Scheme 1, the detection platform comprised of four stages: 1) Homogeneous hybridisation of target and stem loop. 2) Attachment of hybridised DNA to magnetised latex via DIG - anti-DIG bond. 3) Attachment of hybridised DNA to Au-loaded capsules via Au-S bond, following magnetic collection and separation. 4) Quantification by DPASV following acid dissolution. We systematically optimised each of the parameters in this sequence, using the ratio of the DPASV response to 1 pM and 0 pM target DNA (see Supporting Information, Fig. S-7 a-e). The optimised conditions were: anti-DIG (on magnetic latex)-DIG binding time = 20 min, Au nanoparticle (on hollow polyelectrolyte capsule)-thiol binding time = 30 min, target-probe hybridisation time = 40 min, target-probe hybridisation temperature = 40 ^{o}C, probe concentration = 1 nM. Using the platform under optimised parameters we calibrated a 30 mer sequence common to 71 strains of *E. coli* across the concentration range 0.1 aM to 100 pM (see Fig. 3). The calibration curve followed the equation: y (I_{pk}) = 4.08×10^{-7} x (log c [zM]) + 3.30×10^{-6}, r^2 = 0.939, n = 50). Determinations of DNA-free buffer solution (n = 5) gave a mean (μ_b) response of 3.60×10^{-6} A with a standard deviation (σ_b) of 2.07×10^{-7} A. We expect this is due to closed stem loop sequences attaching to the magnetic latex by the DIG group and then the negative phosphate

groups of the stem loop DNA adsorbing to the positively charged PAA capsules. Additionally, a 100 fM non-complementary target (n = 10) gave $\mu_b = 3.94 \times 10^{-6}$ A with σ_b = of 2.29×10^{-7} A. Since the non-complementary target values were higher, we used these as blank responses to calculate the LOD. Defining LOD as the concentration giving a response equal to $\mu_b + 3\,\sigma_b$, (Mocak et al., 1997) results in an LOD of 1.8 aM. This is lower than the lowest of the most recent LODs reported for electrochemical DNA measurement (e.g. 50 aM using Au nanoparticles (Rasheed and Sandhyarani, 2015), 0.2 fM using exonuclease III assisted target recycling with methylene blue as redox indicator (Ren et al., 2015), 1 fM using rolling circle amplification with detection via alkaline phosphatase catalysis (Cheng et al., 2014), 13 aM using horseradish peroxidase labels to generate benzoquinone (Sun et al., 2015), 42 fM using target-catalysed displacement of ferrocene-tagged sequences from stem loop probes (Qian et al., 2014), 4 fM using ferrocene-tagged Au nanoparticles with PCR amplicons (Qiu et al., 2014), 20 fM using exonuclease III assisted target recycling with methylene blue, 10 aM using the change in impedance spectroscopy of $Fe(CN)_6^{3-/4-}$ at an electrode modified by aligned carbon nanotubes modified by Au nanoparticles (Fayazfar et al., 2014), 0.25 fM using exonuclease assisted target recycling with hemin as redox indicator (Wang et al., 2014), with the exception of the report by Benvidi et al. (2014) (3.2 zM using the change in impedance spectroscopy of $Fe(CN)_6^{3-/4-}$ at a reduced graphene-coated electrode). However, this report required 35 PCR cycles to amplify the quantity of genomic DNA being detected.

The selectivity of the platform was examined by measuring the response to 100 fM of complementary target, 1 base mis-match, 3 base mis-match, and non-complementary target. As shown in Fig. 4, the potentially interfering DNA sequences all gave considerably lower responses (< 29% of the response to target).

3.4 Detection of Genomic DNA

We performed genomic DNA extraction using a commercially available kit, having compared this with a simple heat shock procedure and found the kit gave better responses to two different *E. coli* strains (BL21 and ATCC8730, see Supporting Information, Fig. S-8). This was probably because simple heat shock allowed cell materials to enter the sample matrix and thus reduce hybridisation efficiency. The total assay time, including kit-based DNA extraction, was approx. 140 min. We calibrated three strains of *E. coli*, BL 21, ATCC8739, O157:H7, along with *Salmonella enterica serovar* Typhimurium as an example interferent and found detection sensitivity was in the order BL21 > ATCC8739 > O157:H7 >> *Salmonella* (see Supporting Information, Fig. S-9). For the three *E. coli* strains this is in inverse relation to the length of the genome (from the NCBI database, number of base pairs = 4,570,938, 4,746,218 and 5,572,075 for BL21, ATCC8739 and O157:H7

respectively). This is probably because increasing sequence length lowers the efficiency of hybridisation (Ricci et al., 2007) and, for these extremely long sequences, may also reduce the efficiency of label binding, due to steric hindrance. To determine the LOD we used the *Salmonella* response at the highest concentration (10^9 CFU mL^{-1}) as the blank. Five determinations gave $\mu_b = 1.2 \times 10^{-6}$ A and $\sigma_b = 9.3 \times 10^{-8}$ A. From the LOD definition stated previously, the calibrations in Fig. S-9 gave LOD's of 1.8×10^{-3} CFU mL^{-1}, 2.6×10^{-4} CFU mL^{-1} and 2.6×10^{-5} CFU mL^{-1} for the *E. coli* strains BL21, ATCC8739 and O157:H7 respectively. The fact that these LOD are < 1 CFU mL^{-1} reflects the fact that the measurement of genomic DNA applies to the total number of cells present in the sample, while CFU is a measure of only the live cells present. Since the *E. coli* cells were harvested during the log phase, the samples would contain dead cells also.

To examine some of the matrices which may be encountered in the analysis of real samples, we spiked UHT milk (approx. 3% protein (Etzion et al., 2004) and approx. 4% lipids, mainly triglycerides (Garton, 1963)), and fermented palm juice (110 - 130 g L^{-1} carbohydrates, 150 - 190 mg L^{-1} protein, 0.4 -0.8 g L^{-1} fat (Ghosh et al., 2012)) with varying concentrations of *E. coli* from the strains BL21, ATCC8739 and O157:H7, and plotted calibration curves. For each matrix, LODs were determined using μ_b and σ_b from 15 measurements in un-spiked samples. It can be seen from Table 1 that the LODs were in the range 2-4 CFU mL^{-1}. Also as shown in Table 1, this result compares extremely well in comparison with previous electrochemical DNA methods for measuring *E. coli.*, both in terms of assay time and LOD. Recent PCR methods to determine *E. coli.* in water samples has produced LODs of 3-4 cells/L (pre-enrichment, 24 h analysis time, Sen et al., 2011), 15 cells/mL (no pre-enrichment, analysis time not given, Zhang, Y., et al. 2012), 1.8 CFU/100 mL, no pre-enrichment, < 5 h analysis time, Maheux et al., 2011), 50

cells/40 L (> 24 h pre-enrichment, total analysis time not given, Mull and Hill, 2009), and 1 viable cell/100 mL (no pre-enrichment, 3-4 hr analysis time, Heijnen and Medema, 2009).

4. Conclusions

We have described a straightforward and highly sensitive method for the electrochemical detection of genomic DNA. The method is based on a simple utilisation of the solution phase opening of a stem loop probe by hybridisation with target. Two relatively bulky labels, one to enable magnetic collection and the other for electrochemical detection, were attached to the stem loop by DIG-anti-DIG and thiol-Au bonding. Because of the label size, steric hindrance prevented attachment until the loop was straightened by hybridisation with target. The use, for the first time, of seed-mediated deposition onto hollow polyelectrolyte capsules, enabled us to fabricate electrochemical labels containing a high quantity of detectable Au atoms. The use of these labels, combined with magnetic collection resulted in a low LOD for three strains of *E. coli* in real samples, without requiring enzymic amplification by PCR or other means. The platform showed good discrimination against *Salmonella* when present in the same sample matrices.

Acknowledgements

This project received financial support from NANOTEC (grant no. P-110022), and the Higher Education Research Promotion and National Research University Project of Thailand, Office of the Higher Education Commission.

References

Authier, L., Grossiord, C., Brossier, P., Limoges, B., 2000. Anal. Chem. 72, 4450-4456.

Benvidi, A., Rajabzadeh, N., Mazloum-Ardakani, M., Mehdi Heidari, M., Mulchandani, A., 2014. Biosens. Bioelectron. 58, 145-152.

Bonanni, A., Chua, C. K., Zhao, G., Sofer, Z., Pumera, M., 2012. ACS Nano 6, 8546-8551.

Chen, A., Chatterjee, S., 2013. Chem. Soc. Rev. 42, 5425-5438.

Cheng, W., Zhang, W., Yan, Y., Shen, B., Zhu, D., Lei, P., Ding, S., 2014. Biosens. Bioelectron. 62, 274-279.

Davis, F., Higson, S. P. J., In Biosensors for Medical Applications; Higson S. P. J., Ed., Elsevier Inc., Amsterdam, 2012, pp 163-190.

Decher, G., Hong, J. D., 1991. Phys. Chem. Chem. Phys. 95, 1430-1434.

Dong, H. F., Yan, F., Ji, H. X., Wong, D. K. Y., Ju, H. X., 2010. Adv. Funct. Mater. 20, 1173-1179.

Etzion, Y., Linker, R., Cogan, U., Shmulevich, I., 2004. J. Diary Sci. 87, 2779-2788.

Fayazfar, H., Afshar, A., Dolati, M., Dolati, A., 2014. Anal. Chim. Acta 836, 34-44.

Garton, G. A., 1963. J. Lipid Res. 4, 237-254.

Geng, P., Zhang, X., Teng, Y., Fu, Y., Xu, L., Xu, M., Jin, L., Zhang, W., 2011. Biosens. Bioelectron. 26, 3325.

Ghosh, S., Chakraborty, R., Chatterjee, G., Raychaudhuri, U., 2012. Brazil. J. Chem. Eng. 29, 461-472.

Hansen, J. A., Mukhopadhyay, R., Hansen, J. Ø., Gothelf, K. V., 2006. J. Am. Chem. Soc. 128, 3860-3861.

Heijnen, L., Medema, G., 2009. WaterRes. 43, 3124–3132.

Hirsch, L. R., Gobin, A. M., Lowery, A. R., Tam, F., Drezek, R. A., Halas, N. J., West, J. L., 2006. Ann. Biomed. Eng. 34, 15-22.

Li, D., Yan, Y. M., Wieckowska, A., Willner, I., 2007. Chem. Commum. 3544-3546.

Li, H., Sun, Z. Y., Zhong, W. Y., Hao, N., Xu, D. K., Chen, H. Y., 2010. Anal. Chem. 82, 5477-5483.

Lin, L., Liu, Y., Tang, L. H., Li, J. H., 2011. Analyst 136, 4732-4737.

Luo, C., Lei, Y., Yan, L., Yu, T., Li, Q., Zhang, D., Ding, S., Ju, H., 2012. Electroanalysis 24, 1186-1191.

Maheux, A. F., Bissonnette, L., Boissinot, M., Bernier, J-L. T., Huppe, V., Picard, F. J., Berube, E., Bergron, M. G., 2011. Appl. Environ. Microbiol. 77, 6199-6207.

Mocak, J., Bond, A. M., Mitchell, S., Scollary, G., 1997. Pure Appl. Chem. 69, 297-328.

Mull, B., Hill,V.R., 2009. Appl. Environ. Microbiol. 75, 3593–3597.

Ozsoz, M., Ed., Electrochemical DNA Biosensors, Pan Stanford Publishing, Singapore, 2012.

Palecek, E., Fojta, M. In Bioelectronics: From Theory to Applications, Wiley-VCH-Verlag GmbH & Co., 2005, pp 127-192.

Paniel, N., Baudart, J., 2013. Talanta 115, 133-142.

Pinijsuwan, S., Rijiravanich, R., Somasundrum, M., Surareungchai, W., 2008. Anal. Chem. 80, 6779-6784.

Pratiwi, F. W., Rijiravanich, P., Somasundrum, M., Surareungchai, W., 2013. Analyst 138, 5011-5018.

Qian, Y., Wang, C., Gao, F., 2014. Talanta 130, 33-38.

Qiu, L., Qiu, L., Zhou, H., Wu, Z., Shen, G., Yu, R., 2014. New J. Chem. 38, 4711-4715.

Rasheed, P. A., Sandhyarani, N., 2015. Biosens. Bioelectron. 65, 333-340.

Ren, W., Gao, Z. F., Li, N. B., Luo, H. Q., 2015. Biosens. Bioelectron. 63, 153-158.

Ricci, F., Lai, R. Y., Heeger, A. J., Plaxco, K. W., Sumner, J. J., 2007. Langmuir 23, 6827-6834.

Rijiravanich, P., Aoki, K., Chen, J., Surareungchai, W., Somasundrum, M., 2004. Electroanalysis 16, 605-611.

Rijiravanich, P., Somasundrum, M., Surareungchai, W., 2008. Anal. Chem. 80, 3904-3909.

Sanchez-Gaytan, B.L., Park, S-J., 2010. Langmuir 26, 19170-19174.

Sen, K., Sinclair, J. L., Boczek, L., Rice, E. W., 2011. Environ. Sci. Technol. 45, 2250-2256.

Sun, X., Jia, M., Ji, J., Guan, L., Zhang, Y., Tang, L., Li, Z., 2015. Talanta 131, 521-527.

Tadera, K., Minami, Y., Chohchi, M., 2003. Biosci. Biotechnol. Biochem. 67, 1840-1843.

Taton, T. A., Mirkin, C. A., Letsinger, R. L., 2000. Science 289, 1757-1760.

Zhu, Z. Q., Su, Y. Y., Li, J., Li, D., Zhang, J., Song, S. P., Zhao, Y., Li, G. X., Fan, C. H., 2009. Anal Chem. 81, 7660-7666.

Wang, J., Xu, D., Kawde, A-N.; Polsky, R., 2001a. Anal. Chem. 73, 5576-5581.

Wang, J., Polsky, R., Xu, D., 2001b. Langmuir 17, 5739-5741.

Wang, J., Liu, G., Zhu, Q., 2003a. Anal. Chem. 75, 6218-6222.

Wang, J., Lin, G., Jan, M. R., Zhu, Q., 2003b. Electrochem. Commun. 5, 1000-1004.

Wang, S., Lin, L., Jin, H., Yang, T., Bao, W., Huang, S., Wang, J., 2013. Biosens. Bioelectron. 41, 205-210.

Wang, Q., Yang, C., Xiang, Y., Yuan, R., Chai, Y., 2014. Biosens. Bioelectron. 55, 266-271.

Wu, L., Xiong, E., Zhang, X., Zhang, X., Chen, J., 2014. Nano Today 9, 197-211.

Zhang, J., Ting, B. P., Jana, N. R., Gao, Z. Q., Ying, J. Y., 2009. Small 5, 1414-1417.

Zhang, S., Chen, X., Gu, C., Zhang, Y., Xu, J., Bian, Z., Yang, D., Gu, N., 2009. Nanoscale Res. Lett. 4, 70.

Zhang, Y., Riley, L. K., Lin, M., Hu, Z., 2012. Water Res. 46, 2140-2148.

Zhu, Z. Q., Su, Y. Y., Li, J., Li, D., Zhang, J., Song, S. P., Zhao, Y., Li, G. X., Fan, C. H., 2009. Anal Chem. 81, 7660-7666.

http://www.webelements.com/webelements/elements/text/Ag/phys.html.

Legends for Figures

Scheme 1 Schematic representation of the DNA assay. Solution phase hybridisation must occur before the labels can bind to the stem loop probe. Washing steps are performed by holding a magnet below the well plate.

Figure 1 TEM images of seed-decorated hollow PAA capsule before (a) and after the further reduction of Au into the capsules using growth solution volumes of 1 mL (b), 3 mL (c), 5 mL (d), 7 mL (e) and 10 mL (f). (Scale bar = 100 nm for (b) - (d) and 1 µm for (f)).

Figure 2 Quantity of Au atoms in PAA capsules following seed-mediated deposition. Calculated by DPASV measurement of capsules, following dissolution of Au in HBr/Br_2. Error bars show + 1 std. dev. (n = 5).

Figure 3 Calibration of 30 mer target following optimisation. Detection by DPASV (Preconcentration: E_{dep} = -06 V, t_{dep} = 300 s. Differential pulse: E_1 = 0.0 V, E_2 = 1.0 V, modulation time = 0.05 s, interval time = 0.125 s, step potential = 0.00375 V, modulation amplitude = 0.05 V). Error bars show + 1 std. dev. (n = 5).

Figure 4 DPASV response to 100 fM complementary target sequence, one- and three-base mismatch, and non-complementary sequence. DPASV conditions as given in Fig. 5. Error bars show + 1 std. dev. (n = 5).

Table 1 Comparison of limits of detection for *E. coli* in real samples using electrochemical DNA detection.

[a]ASV = anodic stripping voltammetry; DPV = differential pulse voltammetry; CV = cyclic voltammetry.

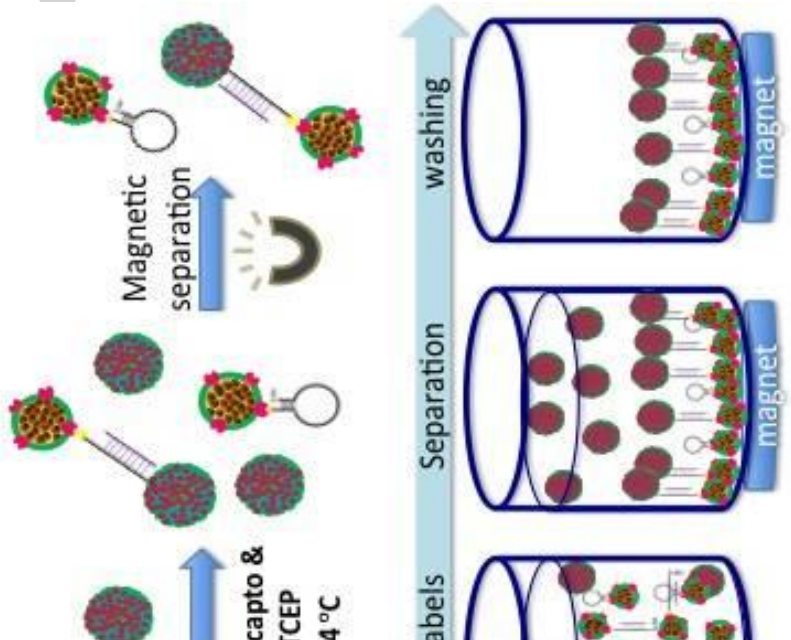

Scheme 1

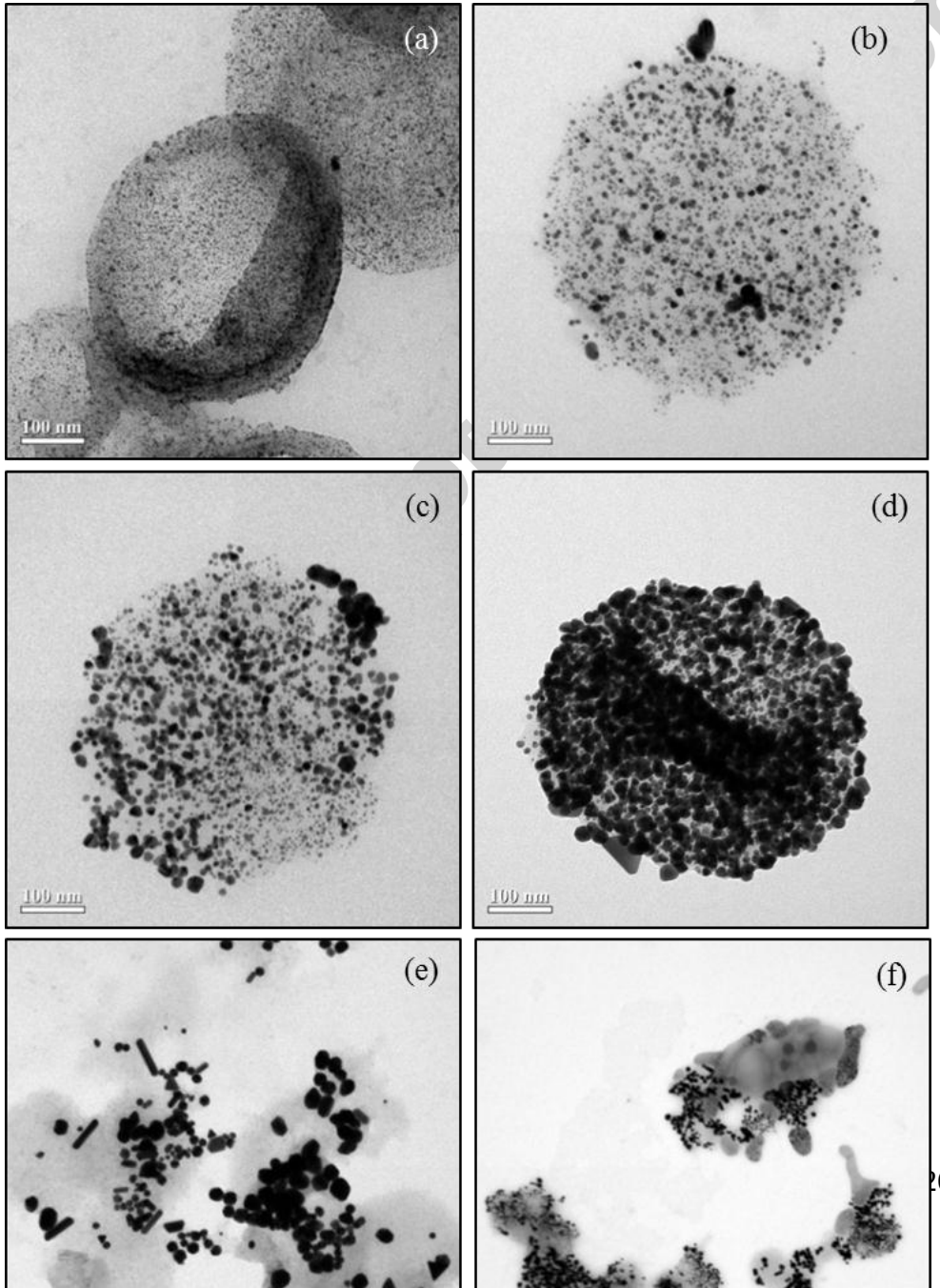
(a)
100 nm
(b)
100 nm
(c)
100 nm
(d)
100 nm
(e)
(f)

Figure 1

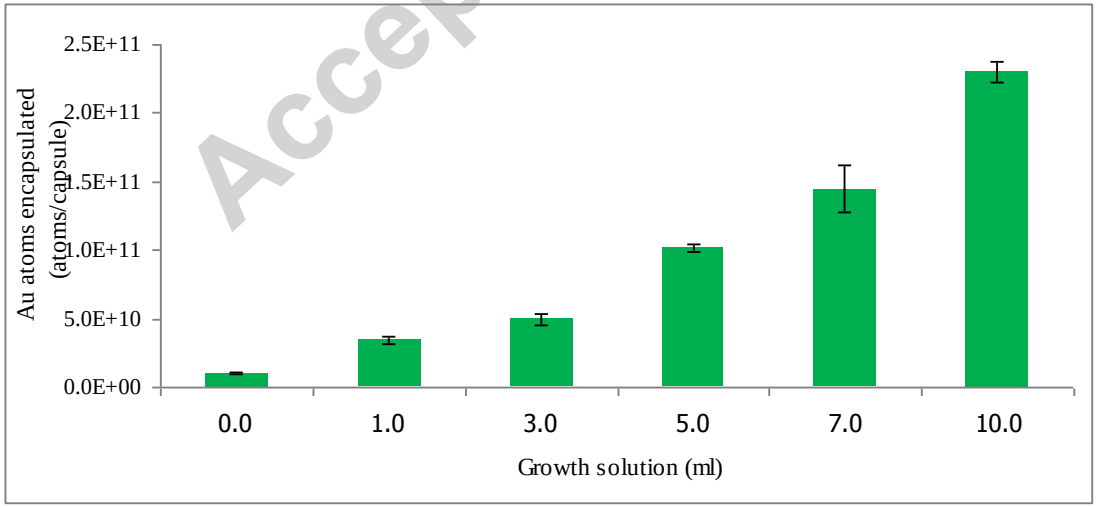

Figure 2

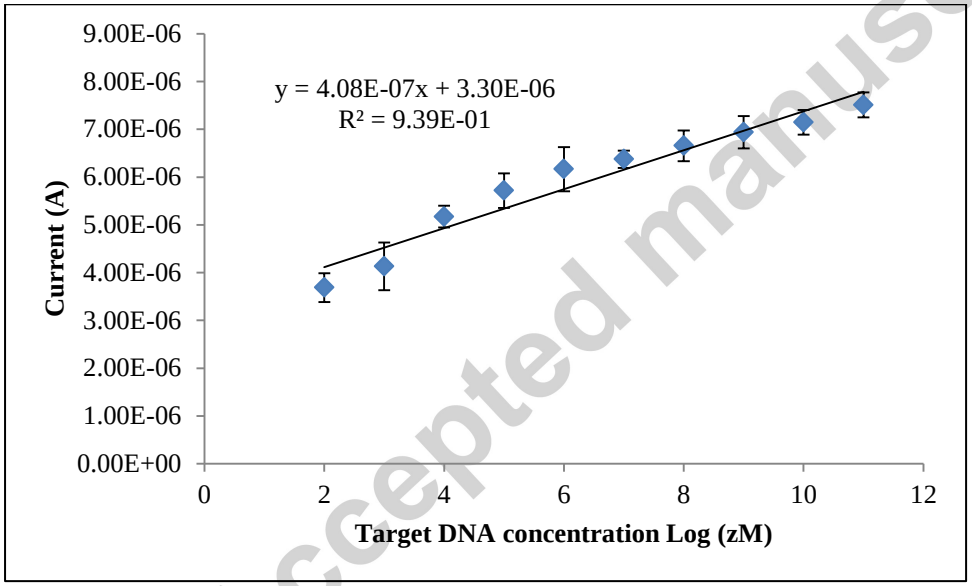

Figure 3

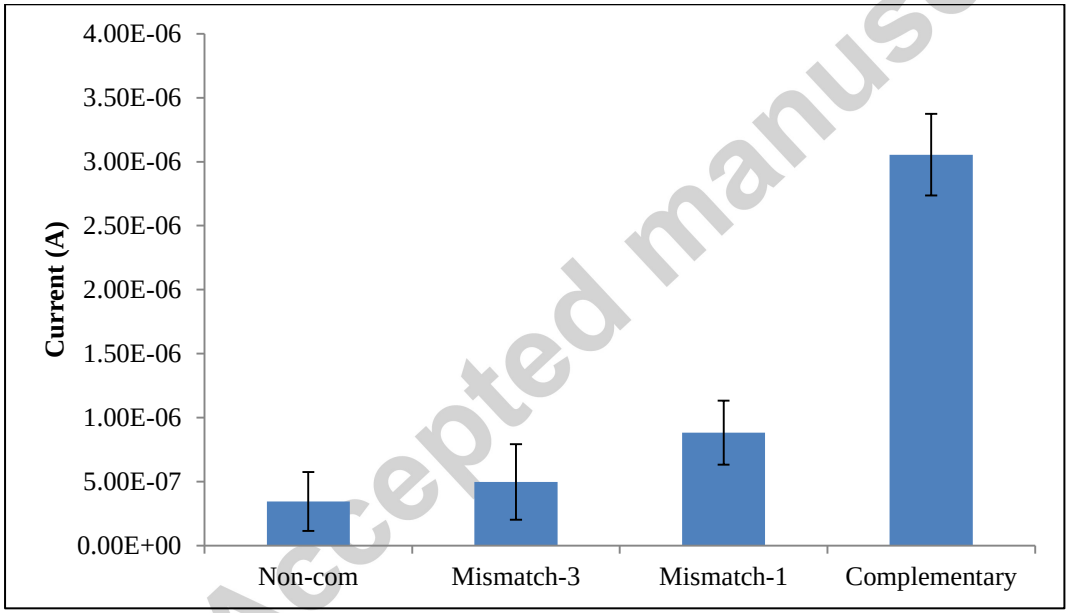

Figure 4

Detection Method[a]	Measured Species	Sample Matrix	Assay Time	LOD (CFU mL^{-1})	Ref.

DPV	α-Napthyl phosphate	Milk	3.5 h	305	Luo et al., 2012
CV	5-Methyl phenazinium methyl sulfate	Seawater	3.5 h	200	Paniel and Baudart, 2013
DPV	Daunomycin	Water	2 h	50	Geng et al., 2011
ASV	Au^{3+} ions	Milk	2.3 h	2.5 (BL21) 2.1 (ATCC8739) 2.6 (O157:H7)	This Work
		Fermented Palm Juice		3.2 (BL21) 3.0 (ATCC8739) 3.7 (O157:H7)	

Table 1

Highlights

- First description of seed mediated metal deposition into hollow polyelectrolyte shells.
- Use of these shells as electrochemical labels.
- Construction of magnetic latex particles as second label.
- Stem loop could capture both labels only after straightening by hybridisation with target.
- High metal content of labels plus magnetic collection provided a low LOD in buffer and real samples.